Veterinary Microbiology 231 (2019) 169–176

Contents lists available at ScienceDirect

Veterinary Microbiology

journal homepage: www.elsevier.com/locate/vetmic

Population divergence of *Pseudomonas aeruginosa* can lead to the coexistence with *Escherichia coli* in animal suppurative lesions

Kelei Zhao[a,*], Jinnan Ma[b], Xinrong Wang[a], Yidong Guo[a], Bisong Yue[b], Yiwen Chu[a,*]

[a] Antibiotics Research and Re-evaluation Key Laboratory of Sichuan Province, Sichuan Industrial Institute of Antibiotics, Chengdu University, Chengdu 610052, China
[b] Key Laboratory of Bio-resources and Eco-environment, Ministry of Education, College of Life Sciences, Sichuan University, Chengdu, 610064, China

ARTICLE INFO

Keywords:
Purulent disease
Forest musk deer
Quorum-sensing
Evolution
Mutation
Coexistence

ABSTRACT

Purulent disease is the main factor that prevents the population increase of forest musk deer in artificial breeding, and especially the intracorporal suppurative lesions in late-stage with complex bacterial communities normally bring more difficulties for veterinary treatment. Although it is well-recognized that *Pseudomonas aeruginosa* and *Escherichia coli* are the two main bacterial pathogens which can be frequently co-isolated from the lung pus of forest musk deer, few studies have explored the interspecific relationship and coexistent mechanism of the two species. In this study, we identified a *P. aeruginosa* strain MYL-2, which harbored a loss-of-function mutation in the central regulator (LasR) of quorum-sensing (QS) system, from the lung pus of a dying forest musk deer with co-infecting *E. coli* strain MYL-58. Interestingly, *P. aeruginosa* MYL-2 could coexist with *E. coli* MYL-58 compared to the dominant role of *lasR*-intact *P. aeruginosa* strain MYL-1 in the competitive experiments. The results of *in vitro* coevolution assay further revealed that the QS-mediated competitive advantage of *P. aeruginosa* MYL-1 would be decreased along with the enrichment of *lasR* mutants in the communities, and *P. aeruginosa* could finally coexist with *E. coli* by forming a relatively stable equilibrium. Therefore, these findings provide an evolutionary explanation for the coexistence of *P. aeruginosa* and *E. coli* in the suppurative lesions of forest musk deer, and may also contribute to further understanding the pathology of animal purulent disease and the development of novel veterinary therapy.

1. Introduction

Forest musk deer (*Moschus berezovskii*) is a kind of economically important ruminant mainly encountered in the southwest of China and categorized as national first-level protected wildlife by Chinese legislation in 2002. The musk secreted by the male deer is a precious traditional Chinese medicine and also an advanced spice used in the perfume industry (Guan et al., 2009; Zhao et al., 2011a). Although the artificial breeding of forest musk deer was started in the 1950s, large-scale breeding has not been performed due to the spread of purulent disease, and suppurative lesions are frequently found in the skin, lung, liver, uterus, and several other tissues of sick or dead deer (Zhao et al., 2011a; Li et al., 2012).

Because of the complex composition of bacterial pathogens in suppurative tissues, debates on the primary pathogen of forest musk deer purulent disease have lasted for several decades (Zhao et al., 2011a, b; Li et al., 2012). By comprehensively characterizing the bacterial species in the pus samples from forest musk deer with different stages of purulent disease, our previous studies find that *Trueperella pyogenes* is the actual primary pathogen which can be detected in all the tested samples. Especially, in comparison to the polymicrobial samples (including *Pseudomonas aeruginosa*, *Escherichia coli*, *Bacucilius cereus*, etc.) from dying or dead forest musk deer, pure *T. pyogenes* is detected in the early-stage abscesses from the body surface of live individuals (Zhao et al., 2011a, b, 2013). Empirically, abscesses on the body surface can be easily diagnosed and cured by artificially removing the pus followed by antibiotic treatment, while the intracorporal suppurative lesions are hard to detect and thus become the leading cause of forest musk deer death.

Bacteria will communicate with neighboring individuals in polymicrobial chronic lesions. The frequent and complicated chemical or physical interactions can integrate local intra/interspecific individuals and facilitate disease progression, and thus clinical therapy by solely targeting the dominant pathogen may not always successful (Short et al., 2014; Pragman et al., 2016). Notably, it has long been found that bacteria can communicate in a process termed quorum-sensing (QS) to

* Corresponding authors at: Antibiotics Research and Re-evaluation Key Laboratory of Sichuan Province, Sichuan Industrial Institute of Antibiotics, Chengdu University, No. 168 Huaguan Road, 610052, Chengdu, Sichuan, PR China.
E-mail addresses: keleizhao@qq.com (K. Zhao), chuyiwen@cdu.edu.cn (Y. Chu).

https://doi.org/10.1016/j.vetmic.2019.03.014
Received 27 December 2018; Received in revised form 19 February 2019; Accepted 11 March 2019

coordinate the production of several extracellular proteases, metabolites, or signal molecules (Fuqua et al., 1994; Schuster et al., 2003). The utilization of these costly and sharable public goods with various functional properties will lead to the establishment of cooperation systems in bacterial populations, and greatly benefit the kin species with similar genotypes at high cell densities (Darch et al., 2012; West and Cooper, 2016). In addition, this altruistic cooperation is susceptible to the exploitation of individuals who do not produce, but benefits from the public goods produced by others (West et al., 2006). By contrast, species with different genotypes are more prone to competing (Foster and Bell, 2012; Mitri and Foster, 2013).

Two forms of competition, resource consumption induced exploitative competition and toxin engendered interference competition, are recognized in the field of ecology (Cornforth and Foster, 2013). Our recent work finds that the subsequently incorporated *P. aeruginosa* and *E. coli* in the intracorporal suppurative lesions of forest musk deer can inhibit the growth and virulence of *T. pyogenes* by using QS signals, and become the dominant pathogens as infection progress (Huang et al., 2018). However, the interspecific relationship between *P. aeruginosa* and *E. coli* still remains largely unknown. Previous study discovers that *P. aeruginosa* can overcome co-cultured *E. coli* in both forms of ecological competition using extracellular factors (such as siderophores and pyocyanin), and *E. coli* may evolve multiple mutations to resist the suppression of *P. aeruginosa* by enhancing the performance of efflux pumps and pyocyanin resistance (Khare and Tavazoie, 2015). In this study, we identified a *P. aeruginosa* QS mutant strain which was co-isolated with *E. coli* from the lung pus of forest musk deer. By performing a series of competitive and *in vitro* evolution experiments, we found that although QS-intact *P. aeruginosa* had higher competitivity than *E. coli*, a relatively stable equilibrium of *P. aeruginosa* and *E. coli* could be reached during coevolution due to the enrichment of QS-mutant *P. aeruginosa*, which could decrease the competitive advantage of *P. aeruginosa* against *E. coli*, and finally lead to the coexistence of both species in the communities.

2. Materials and methods

2.1. Samples and bacterial strains

The 6 *P. aeruginosa* strains (MYL-1 to MYL-6) and 1 *E. coli* MYL58 used in this study were previously isolated and identified from lung pus of 28 dying forest musk deer (Zhao et al., 2011a, b). *P. aeruginosa* MYL-2 and *E. coli* MYL58 were co-isolated from the same lung pus sample. The wild type *P. aeruginosa* PAO1 (WT PAO1), and its isogenic in-frame knockout *lasR* mutant strain (*ΔlasR*) constructed by overlap PCR and conjugation assay, were previously preserved in the laboratory (Deng et al., 2013; Zhao et al., 2014). All the strains were incubated in Luria–Bertani (LB) broth from a single colony and routinely cultured at 37 °C for further use.

2.2. Characterization of P. aeruginosa strains

The full open reading frame of the QS central regulatory gene *lasR* was amplified by using the primer pair 5′-ACGCTGCGGTCTATTG TTA-3′ and 5′-ATCTCGCCCAGCAGTTTT-3′ followed by DNA sequencing. The function of QS system was determined by assessing the growth of *P. aeruginosa* on agar plate of M9 minimal growth medium supplemented with adenosine (0.5%) or sodium caseinate (casein) or skim milk powder (0.5%) as the sole carbon source (Sandoz et al., 2007; Darch et al., 2012). Growth of *P. aeruginosa* in adenosine requires *lasR* regulated nucleoside hydrolase, and the production of *lasR*-regulated extracellular protease elastase can ensure the proliferation of *P. aeruginosa* in digesting casein or milk. The phenotypes of WT PAO1 and the in-frame knockout *lasR* mutant were used as control.

2.3. Culture conditions

The identified QS-intact *P. aeruginosa* strain MYL-1 and *E. coli* MYL-58 were cultured in M9-casein or M9-casamino acids broth at 37 °C with shaking (220 rpm) to monitor their growth status. A fraction of culture liquids at different time-points was used to determine the cell-density by measuring the optical density at 600 nm (OD_{600}).

2.4. Competitive experiments

P. aeruginosa strain MYL-1 or the identified QS-mutant strain MYL-2 were separately mixed with *E. coli* MYL-58 at different ratios (1:99, 50:50, and 99:1) and co-cultured in M9-casein broth with equal initial cell densities ($OD_{600} \approx 0.01$). The proportions of co-cultured *P. aeruginosa* and *E. coli* at different time-points were determined by spreading the appropriately diluted culture liquids on LB agar and LB agar containing 100 μg/ml of ampicillin. Because *P. aeruginosa* had higher ampicillin resistance than *E. coli* (Zhao et al., 2011b), and thus the two species could be separated by the selection of ampicillin. The relative fitness (v) was calculated by comparing the initial and final frequencies of the same species by using the equation $v = \log_{10}[x_1 (1 - x_0)/x_0 (1 - x_1)]$, where x_0 is the initial proportion and x_1 is its final proportion in the population, as described previously with slight modification (Diggle et al., 2007). Specifically, $v > 0$ indicates the growth of one species is faster than the other.

2.5. In vitro evolution evolution

P. aeruginosa MYL-1 and *E. coli* MYL-58 were 1:1 mixed and inoculated ($OD_{600} \approx 0.01$) in 4 ml M9-casein (1%) broth for the *in vitro* evolution assay. The medium was refreshed every other day by transferring an aliquot of cells (400 μl) to another set of culture. At the end of each cycle, 50 μl of culture liquids were appropriately diluted and then transferred onto LB plates. Subsequently, 200 colonies were randomly picked out and transferred onto LB agar supplemented with ampicillin (100 μg/ml) to determine the proportions of *P. aeruginosa* and *E. coli*. A total of 50 *P. aeruginosa* colonies were then transferred onto M9-adenosine and M9-casein/skim milk powder (0.5%) plates to verify their QS abilities. The full region of *lasR* gene was amplified and sequenced as described above. The evolution of pure *P. aeruginosa* was also performed as control. The strains with loss-of-function mutation in *lasR* gene were also confirmed by introducing the recombinant plasmid pAK1900 constitutively expressing LasR (pAK1900-*lasR*) (Deng et al., 2013), followed by phenotypic identification as described above.

2.6. RNA-sequencing and transcriptomic analysis

Bacterial cells from pure *P. aeruginosa* MYL-1 cultures in the *in vitro* evolution assay at day 2 and day 20 were harvested for total RNA isolation using TRIzol reagents (Invitrogen). RNA samples of three independent experiments were well-mixed and sequenced by Novogene Bioinformatics Technology Co., Ltd. (Beijing, China) using prokaryotic strand-specific Illumina-based RNA-Seq technology. The software Tophat2 (Kim et al., 2013) was used to map the clean reads to the reference genome of PAO1 (NCBI accession number: AE004091). The software package Cufflinks (Trapnell et al., 2012) was conducted to get transcriptome assembly and calculate the values of differential gene expression using expected fragments per kilobase of transcript per million fragments (FPKM). Differentially expressed gene with false discovery rate $Q < 0.05$ was thought to be significantly different. Statistics of gene numbers was performed by using VENNY 2.1 (http://bioinfogp.cnb.csic.es/tools/venny/). Heat map was generated by HemI (Deng et al., 2014).

2.7. Quantitative PCR

Quantitative PCR was performed to validate the expression of *lasR*, *lasI*, *rhlR*, *rhlI*, and *lasB* genes of *P. aeruginosa* during the coevolution of *P. aeruginosa* MYL-1 and *E. coli* MYL-58 by using the QIAGEN OneStep RT-PCR Kit (QIAGEN) per the manufacturer's instructions. Specific primer pairs used in this study were accordant to those in our previous study (Zhao et al., 2014). Gene expression was calculated by the $2^{-}\Delta\Delta^{CT}$ method using 16S rRNA as reference (Zhao et al., 2014).

2.8. Statistical analyses

Graphpad Prism version 7.0 (San Diego, CA) was used to conduct data analysis and statistical tests. Data were shown as each replicates or the mean values ± SD of three independent experiments. Data were compared by using two-tailed unpaired *t*-test.

3. Results

3.1. Identification of QS deficient P. aeruginosa strain

Our prior work discovered that QS system played an important role in the competition of *P. aeruginosa* with other bacterial species, and the signal molecule of *P. aeruginosa* QS system could significantly limit the growth of the primary pathogen *T. pyogenes* as purulent disease progresses (Huang et al., 2018; Zhao et al., 2018). In this study, we first checked the gene sequences of the core QS regulator LasR in the 6 *P. aeruginosa* strains from the lung pus of forest musk deer. MYL-2 was found to harbor a transition mutation at the site of 191 bp (A to G) causing amino acid change from tyrosine to cysteine (Table 1 and Supplementary Fig. S1). Accordingly, compared to the normal growth of WT PAO1 and other *lasR*-intact *P. aeruginosa* strains on adenosine and casein/milk plates, MYL-2 showed QS-deficient phenotypes similar with those of the in-frame knockout *lasR* mutant, and the phenotypes of MYL-2 could be restored to QS-positive after introducing the recombinant plasmid pAK1900-*lasR* (Table 1). Because MYL-2 was co-isolated with *E. coli* MYL-58 from the same lung pus sample of a dying forest musk deer, we speculated that QS-deficiency might be related with the coexistence of *P. aeruginosa* and *E. coli* in the lung of forest musk deer.

3.2. P. aeruginosa has a growth advantage over co-cultured E. coli

According to the previously reported role of QS-required condition on selecting *lasR* mutant (Sandoz et al., 2007), the emergence of *lasR* mutant strain MYL-2 might also be due to the development of QS was costly to *P. aeruginosa* population when coexisting with *E. coli* in the lung of forest musk deer. Therefore, in this study, we investigated the interspecific relationship of *P. aeruginosa* and *E. coli* by using the QS-required medium M9-casein. In this medium, *P. aeruginosa* MYL-1 with an intact QS system can digest casein by producing the QS-controlled extracellular elastase encoded by *lasB* (Diggle et al., 2007). As shown in Fig. 1A, both *P. aeruginosa* MYL-1 and *E. coli* MYL-58 could grow in M9-casein broth, and MYL-58 had higher cell density than MYL-1 in stationary phase. Interestingly, when *P. aeruginosa* MYL-1 and *E. coli* MYL-58 were separately cultured using casamino acids (hydrolysates of casein) as the sole carbon source, no significant growth difference was detected between the two species (Fig. 1B). These results indicated that the breakdown of casein by *P. aeruginosa* MYL-1 using QS-controlled elastase was more costly than that by *E. coli* MYL-58, albeit the protease by which used to digest casein was still unclear.

Subsequently, a series of competition experiments was performed to monitor the changes in the proportions of *P. aeruginosa* MYL-1 and *E. coli* MYL-58 in co-culture from different starting ratios. The results showed that when their initial ratios were 1:99 and 1:1, the proportions of MYL-1 were rapidly increased or even became the dominant species with the extension of culture time. On the contrary, the proliferation of MYL-58 was significantly suppressed under the conditions with high initial proportions of MYL-1 (Fig. 2A). Moreover, the relative fitness (growth rate) of MYL-1 was always higher than MYL-58 when they were co-cultured from the mixture with approximately < 75% of MYL-1 (Fig. 2B). These results suggested that *P. aeruginosa* MYL-1 had a growth advantage over co-cultured *E. coli* MYL-58 and could readily invade the population of *E. coli* MYL-58. By contrast, the proportion increase of *lasR* mutant *P. aeruginosa* strain MYL-2 in the co-culture started with 99% of *E. coli* MYL-58 were relatively slow, and MYL-58 could also moderately invade MYL-2 in the co-culture started with 99% of MYL-2. Moreover, no significant proportion change was detected when the two species were co-cultured from a ratio of 1:1, and the relative fitness of MYL-58 was comparable to that of MYL-2 under this co-culture condition (Fig. 2C and D). Therefore, these data suggested that the development of QS system endowed *P. aeruginosa* a growth advantage in the competition with *E. coli*.

Table 1
Characterization of *P. aeruginosa* strains from lung pus of forest musk deer.

Stains	*lasR* mutation[a]	Change[b]	Adenosine[c]	Protease production[c]
MYL-1	None	N/A	+	+
MYL-2	A→G (+191)	Tyr → Cys	–	–
MYL-3	None	N/A	+	+
MYL-4	None	N/A	+	+
MYL-5	None	N/A	+	+
MYL-6	None	N/A	+	+
MYL-2^{com}	None	N/A	+	+
Δ*lasR*	Deletion	N/A	–	–
WT PAO1	None	N/A	+	+

MYL-2^{com}, MYL-2 complemented with plasmid pAK1900-*lasR*.
N/A, not applicable.
[a] Sites of nucleotide mutation relative to translational start site of the *P. aeruginosa* PAO1 *lasR* gene.
[b] Amino acid changes relative to the LasR protein sequence of *P. aeruginosa* PAO1.
[c] +, positive (wild type phenotype); –, negative (defined *lasR* mutant phenotype).

3.3. P. aeruginosa can coexist with E. coli during evolution

We then performed a batch of long-term co-culture assays to explore the interacting dynamics of *P. aeruginosa* and *E. coli* during coevolution. *P. aeruginosa* MYL-1 and *E. coli* MYL-58 were 1:1 mixed and repeatedly subcultured in M9-casein broth by transferring 10% of the culture liquids into fresh medium at 48-h intervals. In accordance to the significant competitive advantage of *P. aeruginosa* MYL-1 in the short-term co-culture with *E. coli* MYL-58 (Fig. 2A and B), MYL-1 was found to be the dominated species in the initial rounds of the *in vitro* coevolution assay (Fig. 3A). Intriguingly, the proportion of *E. coli* MYL-58 began to increase at cycle 3 (day 6) and became comparable to that of *P. aeruginosa* MYL-1 after 8 cycles (16 days), and a stable dynamic equilibrium of the two species was finally formed during further coevolution. These results suggested that *P. aeruginosa* and *E. coli* could indeed coexist in the community, and this might be implicated with the decreased relative fitness of *P. aeruginosa* during evolution.

In checking the population composition of *P. aeruginosa* in each round of the *in vitro* coevolution assay, QS-deficient individuals of *P. aeruginosa* failed to grow on M9-adenosine plate and showed protease-negative phenotype on M9-milk plate were rapidly detected from the co-culture of *P. aeruginosa* MYL-1 and *E. coli* MYL-58 on day 4 (Fig. 3B). As confirmed by DNA sequencing of the full region of *lasR* gene, we identified a *lasR* mutant strain with nonsynonymous mutation at the site of +643 bp resulting in amino acid change from isoleucine to phenylalanine (Supplementary Fig. S1 and Table S1). After day 8, more *lasR* mutants with various mutations such as site mutation and sequence

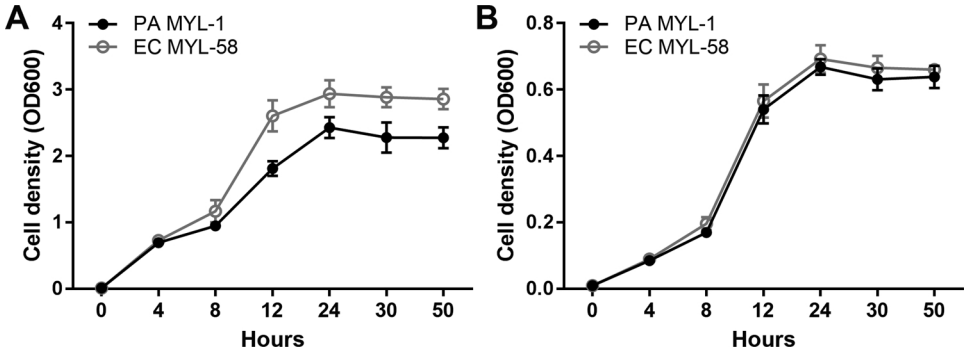

Fig. 1. Growth curves of *P. aeruginosa* MYL-1 and *E. coli* MYL-58 cultured in M9 minimal growth medium containing 0.5% of sodium caseinate (A) or 0.1% of casamino acids (B). The cell-densities of each culture at different time-points were determined by measuring the optical density at 600 nm (OD_{600}). Data shown are mean values ± SD of three independent experiments.

deletion were identified in the population, and the QS-deficient phenotypes of these strains could be restored by introducing the recombinant plasmid pAK1900-*lasR* (Supplementary Table S1). Consistent with the previous finding that *lasR* mutant had a growth advantage when co-cultured with QS-intact *P. aeruginosa* by escaping from QS-imposed metabolic burden (Diggle et al., 2007; Sandoz et al., 2007; Zhao et al., 2016), the frequency of *lasR* mutants rapidly increased in the polymorphic populations once emerged, and the final proportion of which in the dynamic equilibrium was comparable to that in pure *P. aeruginosa* MYL-1 culture (Fig. 3B and Supplementary Fig. S2). Therefore, our results here showed that the population divergence of *P. aeruginosa* could also happen during the coevolution with *E. coli*, and this finding combined with the weak competitivity of *P. aeruginosa lasR* mutants against *E. coli*, providing an explanation for the coexistence of *P. aeruginosa* and *E. coli* in the communities during evolution.

3.4. QS-regulation of *P. aeruginosa* will be decreased during evolution

To probe the underlying mechanism for the decreased competitivity of *P. aeruginosa* during evolution, RNA-sequencing was conducted to find out the transcriptional change of evolved *P. aeruginosa*. The results of comparative-transcriptomic analysis showed that a total of 726 down-regulated genes significantly enriched in bacterial chemotaxis and 1176 up-regulated genes significantly enriched in ABC transporters and sulfur metabolism were detected in the evolved *P. aeruginosa* MYL-1 at day 20 (dynamic equilibrium) (Supplementary Table S2 and Fig. S3). We noticed that the *pvd* operon for the biosynthesis of siderophore pyoverdine, the *pqsB* and *pqsC* genes in synthesizing the *Pseudomonas* quinolone signal (PQS), and the *phzB1*and *phzH* genes in synthesizing the phenazine molecule pyocyanin, which had been reported to play key roles in overcoming co-cultured *E. coli* (Khare and Tavazoie, 2015), were up-regulated during evolution. Considering the role of *P. aeruginosa* QS system in directing the coexistence with *E. coli* (Fig. 2 and 3), we further explored the transcriptional changes of QS-related genes. When the significantly down-regulated genes of evolved MYL-1 were applied to the regulatory profile of *P. aeruginosa* QS system (Schuster et al., 2003), about 38% of QS-activated genes (111 out of 292) including the central regulatory genes *lasR/rhlR* and corresponding signal synthesis genes *lasI/rhlI* and the elastase-encoding gene *lasB* (2- to 4-fold decline) were obtained (Fig. 4 and Table 2). The expression of these five genes of *P. aeruginosa* were all significantly down-regulated in the coevolution of MYL-1 and MYL-58 at day 20 compared to those at day 2 (Supplementary Fig. S4). Therefore, the coexistence of *P. aeruginosa* and *E. coli* during evolution might be jointly directed by the toxicity of *P. aeruginosa* extracellular metabolites on *E. coli* (Khare and Tavazoie, 2015), and the enrichment of *lasR* mutants which could decrease the QS-mediated competitivity of *P. aeruginosa*.

4. Discussion

Intracorporal suppurative lesions of economically important animals are normally chronic and hard to be diagnosed in time. The

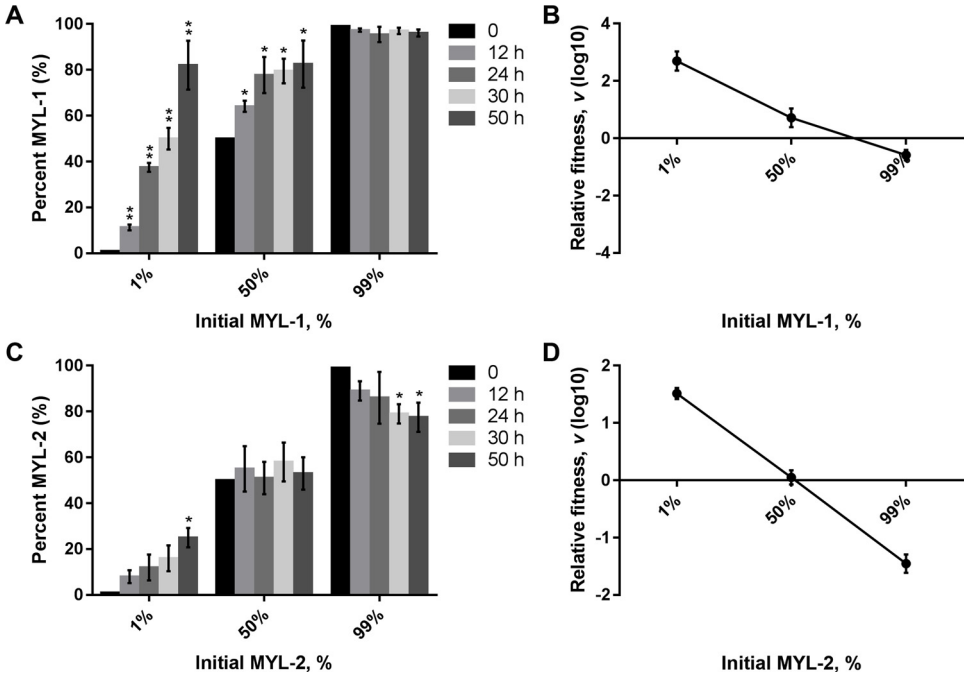

Fig. 2. Competitive experiments. (A) Proportion changes of *P. aeruginosa* MYL-1 when co-cultured with *E. coli* MYL-58 in M9-casein broth from different initial ratios. (B) Relative fitness of *P. aeruginosa* MYL-1 when co-cultured with *E. coli* MYL-58 from different initial ratios for 50 h. (C) Proportion changes of *P. aeruginosa* MYL-2 (harboring a loss-of-function mutation in *lasR* gene) when co-cultured with *E. coli* MYL-58 in M9-casein broth from different initial ratios. (D) Relative fitness of *P. aeruginosa* MYL-2 when co-cultured with *E. coli* MYL-58 from different initial ratios for 50 h. Data shown are mean values ± SD of three independent experiments. Percentages of each strain at different time-point were compared to that at 0 h using two-tailed unpaired *t*-test. *, $P < 0.05$; **, $P < 0.01$. $v > 0$ indicates the growth of *P. aeruginosa* is faster than *E. coli*.

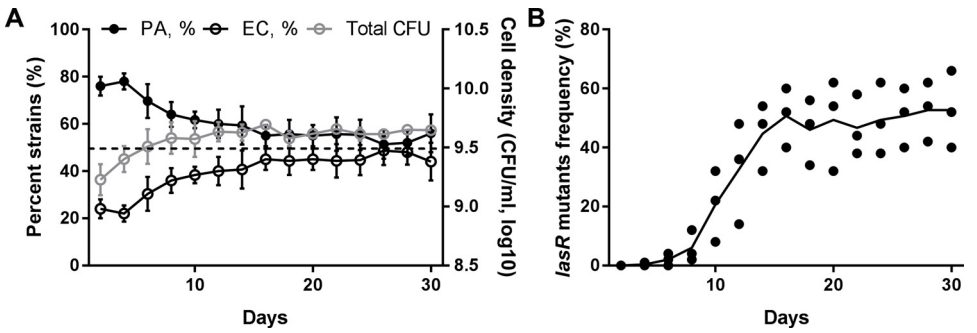

Fig. 3. *In vitro* coevolution. (A) Proportion changes of *P. aeruginosa* MYL-1 (solid dots) and *E. coli* MYL-58 (blank dots) and total cell densities (blank gray dots) during coevolution of both species in M9-casein broth from an initial ratio of 1:1. Data shown are mean values ± SD of three independent experiments. (B) Proportions of *P. aeruginosa lasR* mutants during the coevolution experiment in panel (A). Data shown are the means (lines) for the replicates (symbols) of three independent experiments.

polymicrobial feature of these diseases brings the most serious challenge for veterinary treatment and economical increase, and increasing evidences also suggest that bacterial interspecific communications can promote disease progression in a synergic manner (Zhao et al., 2011b; Short et al., 2014; Pragman et al., 2016). In this study, based on the previous characterization of bacterial communities in the suppurative tissues of forest musk deer, we found that although the development of QS system endowed *P. aeruginosa* with higher relative fitness in competing with *E. coli*, the competitive advantage of *P. aeruginosa* would be decreased along with the enrichment of QS-deficient individuals, and this divergence in *P. aeruginosa* population enabled the coexistence with *E. coli* during further evolution.

P. aeruginosa evolved several kinds of capacities to dominate the competition with other species (Tashiro et al., 2013). Especially, the discovery of QS system provided a great convenience for characterizing bacterial cell-cell interactions (Nealson et al., 1970; Eberhard et al., 1981; Fuqua et al., 1994). The interactions between *P. aeruginosa* and *Staphylococcus aureus*, which normally coexist in the lung of cystic fibrosis patients with other bacterial pathogens, had been characterized in much more details (Hotterbeekx et al., 2017). The presence of *S. aureus* could increase the PQS pathway induced virulence of *P. aeruginosa*, while the QS-controlled extracellular metabolites of *P. aeruginosa*

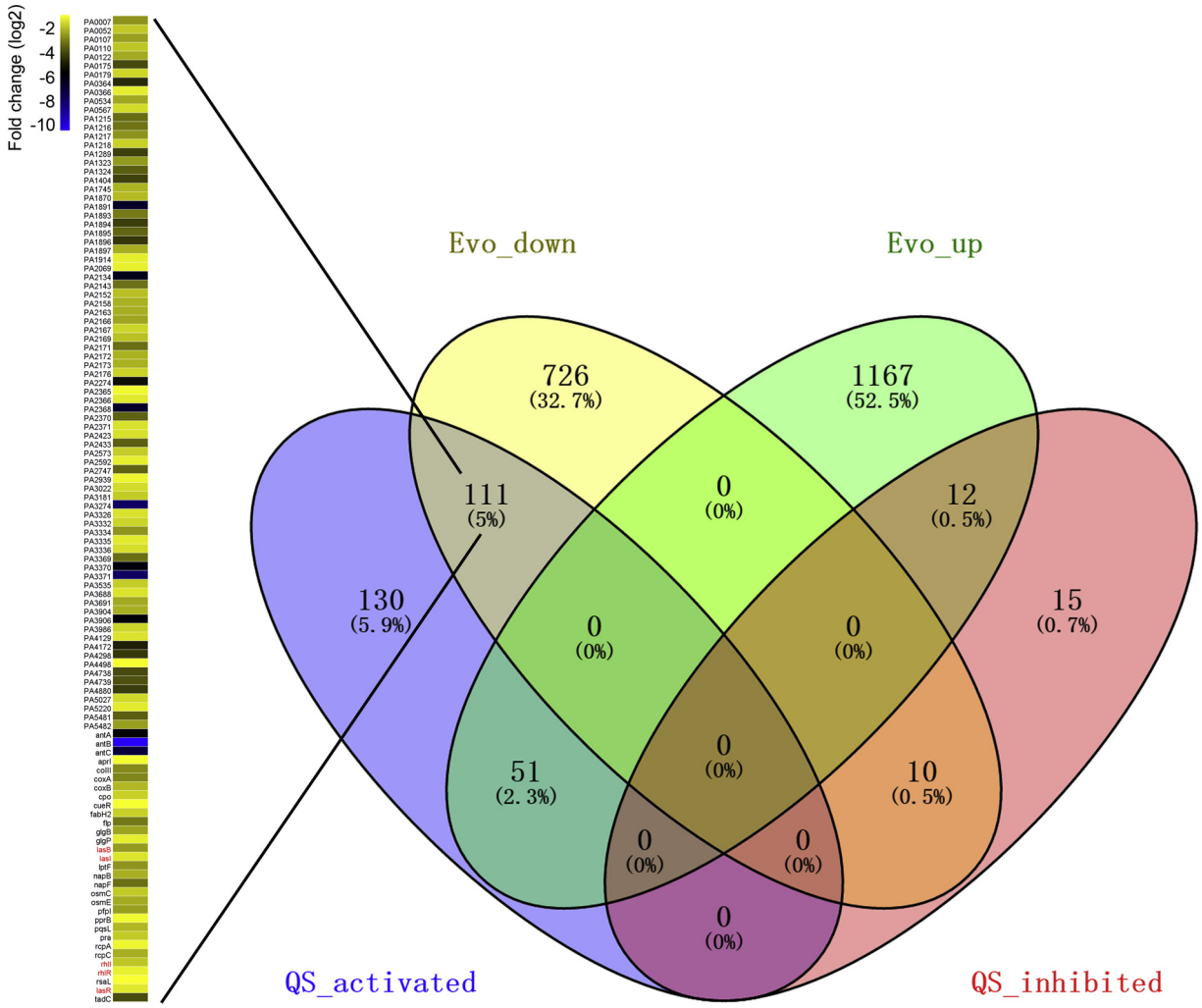

Fig. 4. The QS-regulation of *P. aeruginosa* was decreased during evolution. The global transcriptional profile of repeatedly (48-h intervals) subcultured *P. aeruginosa* MYL-1 in M9-casein broth at day 20 was compared to that of day 2. The significantly down-regulated genes were applied to the regulatory profile of *P. aeruginosa* QS system (Δ*lasR-rhlR vs.* wild type) published by Schuster et al. (2003) using VENNY 2.1.

Table 2
Significantly down-regulated QS-related genes of *P. aeruginosa* during evolution in M9-casein broth. Data shown are false discovery rate $Q < 0.05$ as generated and calculated by the software package Cufflinks.

Gene_id	20 days	2 day	FC (log2)*	Q value	Gene	Description
PA0007	221.03121	1334.1631	−2.5936	8.61E-95	PA0007	hypothetical protein
PA0052	33.489577	118.33904	−1.8211	2.05E-05	PA0052	hypothetical protein
PA0059	46.885408	164.21368	−1.8084	1.16E-06	osmC	osmotically inducible protein OsmC
PA0105	415.27076	1743.8208	−2.0701	1.45E-74	coxB	cytochrome C oxidase subunit II
PA0106	107.16665	747.72744	−2.8027	3.42E-62	coxA	cytochrome C oxidase subunit I
PA0107	20.093746	106.94343	−2.412	2.40E-08	PA0107	cytochrome C oxidase assembly protein
PA0108	73.67707	485.04398	−2.7188	9.44E-39	coIII	cytochrome C oxidase subunit III
PA0110	93.770816	341.28396	−1.8638	1.38E-12	PA0110	hypothetical protein
PA0122	1801.7393	8561.3184	−2.2484	3.46E-14	PA0122	hypothetical protein
PA0175	13.395831	184.08296	−3.7805	2.58E-25	PA0175	chemotaxis protein methyltransferase
PA0179	281.31245	875.41673	−1.6378	3.93E-20	PA0179	two-component response regulator
PA0355	26.791662	143.46783	−2.4209	1.42E-10	pfpI	protease PfpI
PA0364	6.6979154	137.62392	−4.3609	2.34E-22	PA0364	oxidoreductase
PA0366	93.770816	234.92492	−1.325	0.0004836	PA0366	coniferyl aldehyde dehydrogenase
PA0534	133.95831	657.43913	−2.2951	6.26E-37	PA0534	hypothetical protein
PA0567	40.187493	120.09221	−1.5793	0.0003885	PA0567	hypothetical protein
PA1173	6.6979154	30.388298	−2.1817	0.0024678	napB	cytochrome C protein NapB
PA1176	13.395831	119.50782	−3.1572	9.95E-14	napF	ferredoxin protein NapF
PA1215	53.583323	488.25813	−3.1878	6.95E-51	PA1215	hypothetical protein
PA1216	46.885408	390.95714	−3.0598	1.47E-38	PA1216	hypothetical protein
PA1217	87.072901	523.02935	−2.5866	6.13E-38	PA1217	2-isopropylmalate synthase
PA1218	46.885408	152.81807	−1.7046	1.34E-05	PA1218	hypothetical protein
PA1250	160.74997	350.6342	−1.1251	0.0037019	aprI	alkaline proteinase inhibitor AprI
PA1289	6.6979154	102.5605	−3.9366	1.27E-15	PA1289	hypothetical protein
PA1323	107.16665	601.92205	−2.4897	3.02E-40	PA1323	hypothetical protein
PA1324	40.187493	435.663	−3.4384	7.35E-51	PA1324	hypothetical protein
PA1404	6.6979154	101.09953	−3.9159	2.39E-15	PA1404	hypothetical protein
PA1430	408.57284	1068.2655	−1.3866	9.94E-14	lasR	transcriptional regulator
PA1431	676.48946	1397.2773	−1.0465	6.77E-05	rsaL	regulatory protein RsaL
PA1432	1145.3435	3101.6517	−1.4373	9.47E-42	lasI	acyl-homoserine-lactone synthase
PA1745	13.395831	57.270253	−2.096	0.0002145	PA1745	hypothetical protein
PA1870	20.093746	80.938062	−2.0101	4.51E-05	PA1870	hypothetical protein
PA1891	0	37.693177	−6.2362	8.24E-09	PA1891	hypothetical protein
PA1893	113.86456	900.8377	−2.9839	3.13E-83	PA1893	hypothetical protein
PA1894	26.791662	428.06592	−3.998	3.07E-60	PA1894	hypothetical protein
PA1895	60.281239	599.0001	−3.3128	9.70E-66	PA1895	hypothetical protein
PA1896	26.791662	465.7591	−4.1197	1.56E-67	PA1896	hypothetical protein
PA1897	100.46873	460.79178	−2.1974	4.74E-24	PA1897	hypothetical protein
PA1914	93.770816	232.29516	−1.3087	0.0006787	PA1914	hypothetical protein
PA2069	455.45825	1098.3616	−1.27	5.13E-10	PA2069	carbamoyl transferase
PA2134	0	31.557078	−5.9799	1.18E-07	PA2134	hypothetical protein
PA2143	6.6979154	59.023424	−3.1395	9.47E-08	PA2143	hypothetical protein
PA2144	66.979154	166.84344	−1.3167	0.0023484	glgP	glycogen phosphorylase
PA2152	40.187493	155.15563	−1.9489	1.83E-07	PA2152	trehalose synthase
PA2153	20.093746	102.26831	−2.3475	1.03E-07	glgB	1%2C4-alpha-glucan branching protein GlgB
PA2158	6.6979154	29.803907	−2.1537	0.002921	PA2158	alcohol dehydrogenase
PA2163	20.093746	90.872697	−2.1771	3.01E-06	PA2163	4-alpha-glucanotransferase
PA2166	33.489577	168.88881	−2.3343	2.62E-11	PA2166	hypothetical protein
PA2167	46.885408	148.72734	−1.6655	3.07E-05	PA2167	hypothetical protein
PA2169	13.395831	51.134155	−1.9325	0.0011126	PA2169	hypothetical protein
PA2171	13.395831	118.92343	−3.1502	1.25E-13	PA2171	hypothetical protein
PA2172	26.791662	118.33904	−2.1431	2.46E-07	PA2172	hypothetical protein
PA2173	13.395831	59.023424	−2.1395	0.0001303	PA2173	hypothetical protein
PA2176	26.791662	85.320989	−1.6711	0.0008063	PA2176	hypothetical protein
PA2274	0	15.778539	−4.9799	0.0001466	PA2274	hypothetical protein
PA2365	160.74997	356.47811	−1.149	0.0022169	PA2365	hypothetical protein
PA2366	288.01036	746.55866	−1.3741	6.78E-10	PA2366	uricase
PA2368	0	38.861957	−6.2803	4.99E-09	PA2368	hypothetical protein
PA2370	13.395831	137.03953	−3.3547	9.38E-17	PA2370	hypothetical protein
PA2371	254.52079	713.5406	−1.4872	1.95E-12	PA2371	ClpA/B-type protease
PA2423	107.16665	305.34395	−1.5106	9.68E-07	PA2423	hypothetical protein

(*continued on next page*)

Table 2 (*continued*)

Gene_id	20 days	2 day	FC (log2)*	*Q* value	Gene	Description
PA2433	33.489577	350.34201	−3.387	2.32E-40	PA2433	hypothetical protein
PA2512	80.374985	3107.2034	−5.2727	1.18E-16	antA	anthranilate dioxygenase large subunit
PA2513	0	386.28201	−9.5935	2.43E-59	antB	anthranilate dioxygenase small subunit
PA2514	13.395831	1295.3012	−6.5954	8.10E-240	antC	anthranilate dioxygenase reductase
PA2573	221.03121	753.57134	−1.7695	5.05E-22	PA2573	chemotaxis transducer
PA2592	247.82287	614.48644	−1.3101	3.21E-07	PA2592	spermidine/putrescine-binding protein
PA2717	26.791662	87.366355	−1.7053	0.0005266	cpo	chloroperoxidase
PA2747	127.26039	1266.6661	−3.3152	1.24E-137	PA2747	hypothetical protein
PA2939	495.64574	1142.7753	−1.2052	2.66E-08	PA2939	aminopeptidase
PA3022	167.44789	495.56301	−1.5654	8.91E-11	PA3022	hypothetical protein
PA3181	13.395831	46.459032	−1.7942	0.0034896	PA3181	2-dehydro-3-deoxy-phosph ogluconate aldolase
PA3274	0	79.769281	−7.3178	3.26E-16	PA3274	hypothetical protein
PA3326	582.71864	1619.6378	−1.4748	6.31E-25	PA3326	ATP-dependent Clp protease proteolytic subunit
PA3332	60.281239	190.80345	−1.6623	3.79E-06	PA3332	hypothetical protein
PA3333	174.1458	571.24155	−1.7138	9.98E-16	fabH2	3-oxoacyl-ACP synthase III
PA3334	33.489577	199.8615	−2.5772	1.35E-15	PA3334	acyl carrier protein
PA3335	187.54163	483.29081	−1.3657	5.74E-07	PA3335	hypothetical protein
PA3336	180.84372	521.56838	−1.5281	1.84E-10	PA3336	major facilitator superfamily transporter
PA3369	26.791662	239.60004	−3.1608	1.47E-25	PA3369	hypothetical protein
PA3370	0	24.252199	−5.6	3.03E-06	PA3370	hypothetical protein
PA3371	0	80.061476	−7.323	2.92E-16	PA3371	hypothetical protein
PA3476	288.01036	1052.7792	−1.87	4.93E-35	rhlI	acyl-homoserine-lactone synthase
PA3477	596.11447	1444.6129	−1.277	7.95E-13	rhlR	transcriptional regulator RhlR
PA3535	100.46873	342.45274	−1.7692	4.20E-11	PA3535	serine protease
PA3688	140.65622	389.20396	−1.4684	2.04E-07	PA3688	hypothetical protein
PA3691	221.03121	1054.5324	−2.2543	6.24E-56	PA3691	hypothetical protein
PA3692	207.63538	1237.1543	−2.5749	9.28E-87	lptF	outer membrane porin F
PA3724	3054.2494	17030.011	−2.4792	3.16E-17	lasB	elastase LasB
PA3904	26.791662	121.55319	−2.1817	9.98E-08	PA3904	hypothetical protein
PA3906	0	21.330247	−5.4148	1.13E-05	PA3906	hypothetical protein
PA3986	154.05206	486.79715	−1.6599	1.50E-12	PA3986	hypothetical protein
PA4129	187.54163	514.55569	−1.4561	6.20E-09	PA4129	hypothetical protein
PA4172	0	12.272197	−4.6173	0.000768	PA4172	nuclease
PA4190	33.489577	140.54588	−2.0693	8.36E-08	pqsL	monooxygenase
PA4296	281.31245	628.51181	−1.1598	0.0001009	pprB	two-component response regulator PprB
PA4298	0	8.4736599	−4.083	0.0046547	PA4298	hypothetical protein
PA4300	6.6979154	88.827331	−3.7292	4.65E-13	tadC	type II secretion system protein TadC
PA4304	93.770816	215.93223	−1.2034	0.0046014	rcpA	type II/III secretion system protein
PA4305	87.072901	395.63226	−2.1839	1.19E-20	rcpC	hypothetical protein
PA4306	348.2916	2795.7234	−3.0049	6.59E-259	flp	type IVb pilin Flp
PA4498	495.64574	1061.8372	−1.0992	3.09E-05	PA4498	metallopeptidase
PA4590	46.885408	161.58393	−1.7851	2.09E-06	pra	protein activator
PA4738	13.395831	182.32979	−3.7667	5.52E-25	PA4738	hypothetical protein
PA4739	87.072901	1098.0694	−3.6566	7.58E-137	PA4739	hypothetical protein
PA4778	200.93746	424.85178	−1.0802	0.0049977	cueR	protein CueR
PA4876	113.86456	530.33423	−2.2196	5.24E-28	osmE	OsmE family transcriptional regulator
PA4880	20.093746	329.01176	−4.0333	4.13E-47	PA4880	bacterioferritin
PA5027	388.4791	1189.5265	−1.6145	1.80E-25	PA5027	hypothetical protein
PA5220	154.05206	395.04787	−1.3586	5.86E-06	PA5220	hypothetical protein
PA5481	46.885408	498.19276	−3.4095	2.95E-57	PA5481	hypothetical protein
PA5482	46.885408	251.58004	−2.4238	4.76E-17	PA5482	hypothetical protein

* Log2 fold change of gene expression levels at day 20 compared to day 2.

were harmful to the growth of *S. aureus*. Intriguingly, the QS-deficient *P. aeruginosa* individuals were capable of coexisting with *S. aureus* or even evolved a commensal-like interaction (Korgaonkar et al., 2013; Frydenlund Michelsen et al., 2016; Hotterbeekx et al., 2017; Zhao et al., 2018). Khare and Tavazoie (2015) showed that in addition to the innate advantage in iron acquisition, *P. aeruginosa* could directly inhibit the growth of *E. coli* by secreting the toxic molecule pyocyanin, and the *de novo* biosynthesis of pyocyanin was multiply regulated by the *las*, *rhl*, and *pqs* QS systems (Higgins et al., 2018). Our current study found that the growth of *E. coli* could be significantly suppressed by the presence of *P. aeruginosa* with an intact QS system (Fig. 2), and thus also emphasized the role of QS system in enhancing the competitivity of *P. aeruginosa* during interspecific interactions.

However, it seemed that a robust QS-regulation was not always

required for the fitness of *P. aeruginosa*, because this energy-intensive process would cause a social competition for the costly public goods under nutrient-decreasing condition and promote the selection of QS-deficient individuals during evolution (Sandoz et al., 2007; Eldar, 2011; Zhao et al., 2016). A recent study by Özkaya et al. (2018) developed a three-way public goods game to investigate the evolutionary dynamics of polymorphic populations using *P. aeruginosa* as a model. They found that the invasion of pyoverdine-deficient mutants (QS active) to QS-deficient mutants (pyoverdine positive) was able to prevent the population collapse caused by QS mutants, but depending on the type and composition of resources available for growth. The outcome of this game was similar to our finding that the incorporation of *P. aeruginosa lasR* mutants, which decreased the relative fitness of WT individuals (Diggle et al., 2007), could reconcile the competition between *P. aeruginosa* and *E. coli* (Figs. 2 and 3). Moreover, the decreased competitivity of *P. aeruginosa* during evolution was consistent with the result of transcriptomic analysis, which revealed that the expression levels of 38% of genes positively regulated by *P. aeruginosa* QS system were declined in the evolved population (Fig. 4). Therefore, compared with the dominated role of *P. aeruginosa* in short-period co-culture with *E. coli*, the subsequently formed dynamic equilibrium of the proportions of the two species might be due to the growth advantage of *E. coli* was comparable to *P. aeruginosa* with diverged population structure.

Noteworthily, although *P. aeruginosa lasR* mutant strain and *E. coli* could be co-isolated from the lung pus of forest musk deer, the potential mutations in other sites and nutrient difference between *in vitro* culture and in the host tissues might bias the outcome of real-life bacterial game (Harrison et al., 2017; Özkaya et al., 2018), and the functions of bacterial chemotaxis and membrane transporter-depended metabolite exchange might also contribute to the interspecific coexistence in the local microcommunity (Short et al., 2014). Therefore, further whole-genome sequencing based genetic characterizations of *P. aeruginosa* MYL-2 and *E. coli* MYL-58, and more detailed studies using infection-mimicking media or animal models would help to confirm the interacting dynamics between *P. aeruginosa* and *E. coli* in the host tissues.

In conclusion, our current study provides an evolutionary explanation for the coexistence of *P. aeruginosa* and *E. coli* during evolution, may remarkably facilitate the understanding of the pathology of chronic infections involving both species, and shed new light on the development of veterinary therapies.

Conflict of interest

The authors declare no conflict of interest exists.

Acknowledgments

This work was supported by the National Natural Science Foundation of China (31700111), the Science and Technology Bureau of Chengdu Municipal Government for “Collaboration and Innovation on New Antibiotic Development and Industrialization” (2016-XT00-00023-GX) and the Sichuan Science and Technology Program (2018HH0007).

Appendix A. Supplementary data

Supplementary material related to this article can be found, in the online version, at doi:https://doi.org/10.1016/j.vetmic.2019.03.014.

References

Cornforth, D.M., Foster, K.R., 2013. Competition sensing: the social side of bacterial stress responses. Nat. Rev. Microbiol. 11, 285–293.
Darch, S.E., West, S.A., Winzer, K., Diggle, S.P., 2012. Density-dependent fitness benefits in quorum-sensing bacterial populations. Proc. Natl. Acad. Sci. U.S.A. 109, 8259–8263.
Deng, X., Weerapana, E., Ulanovskaya, O., Sun, F., Liang, H., Ji, Q., Ye, Y., Fu, Y., Zhou, L., Li, J., Zhang, H., Wang, C., Alvarez, S., Hicks, L.M., Lan, L., Wu, M., Cravatt, B.F., He, C., 2013. Proteome-wide quantification and characterization of oxidation-sensitive cysteines in pathogenic bacteria. Cell Host Microbe 13, 358–370.
Deng, W., Wang, Y., Liu, Z., Cheng, H., Xue, Y., 2014. HemI: a toolkit for illustrating heatmaps. PLoS One 9, e111988.
Diggle, S.P., Griffin, A.S., Campbell, G.S., West, S.A., 2007. Cooperation and conflict in quorum-sensing bacterial populations. Nature 450, 411–414.
Eberhard, A., Burlingame, A.L., Eberhard, C., Kenyon, G.L., Nealson, K.H., Oppenheimer, N.J., 1981. Structural identification of autoinducer of *Photobacterium fischeri* luciferase. Biochemistry 20, 2444–2449.
Eldar, A., 2011. Social conflict drives the evolutionary divergence of quorum sensing. Proc. Natl. Acad. Sci. U.S.A. 108, 13635–13640.
Foster, K.R., Bell, T., 2012. Competition, not cooperation, dominates interactions among culturable microbial species. Curr. Biol. 22, 1845–1850.
Frydenlund Michelsen, C., Hossein Khademi, S.M., Krogh Johansen, H., Ingmer, H., Dorrestein, P.C., Jelsbak, L., 2016. Evolution of metabolic divergence in *Pseudomonas aeruginosa* during long-term infection facilitates a proto-cooperative interspecies interaction. ISME J. 10, 1323–1336.
Fuqua, W.C., Winans, S.C., Greenberg, E.P., 1994. Quorum sensing in bacteria: The LuxR-LuxI family of cell density-responsive transcriptional regulators. J. Bacteriol. 176, 269–275.
Guan, T.L., Zeng, B., Peng, Q.K., Yue, B.S., Zou, F.D., 2009. Microsatellite analysis of the genetic structure of captive forest musk deer populations and its implication for conservation. Biochem. Syst. Ecol. 37, 166–173.
Harrison, F., McNally, A., da Silva, A.C., Heeb, S., Diggle, S.P., 2017. Optimised chronic infection models demonstrate that siderophore’ cheating’ in *Pseudomonas aeruginosa* is context specific. ISME J. 11, 2492–2509.
Higgins, S., Heeb, S., Rampioni, G., Fletcher, M.P., Williams, P., Cámara, M., 2018. Differential regulation of the phenazine biosynthetic operons by quorum sensing in *Pseudomonas aeruginosa* PAO1-N. Front. Cell. Infect. Microbiol. 8, 252.
Hotterbeekx, A., Kumar-Singh, S., Goossens, H., Malhotra-Kumar, S., 2017. In vivo and in vitro interactions between Pseudomonas aeruginosa and Staphylococcus spp. Front. Cell. Infect. Microbiol. 7, 106.
Huang, T., Song, X., Zhao, K., Jing, J., Shen, Y., Zhang, X., Yue, B., 2018. Quorum-sensing molecules N-Acyl homoserine lactones inhibit *Trueperella pyogenes* infection in mouse model. Vet. Microbiol. 213, 89–94.
Khare, A., Tavazoie, S., 2015. Multifactorial competition and resistance in a two-species bacterial system. PLoS Genet. 11, e1005715.
Kim, D., Pertea, G., Trapnell, C., Pimentel, H., Kelley, R., Salzberg, S.L., 2013. TopHat2: accurate alignment of transcriptomes in the presence of insertions, deletions and gene fusions. Genome Biol. 14, R36.
Li, Q., Yan, Q., Kang, J., Li, P., Xiong, W., 2012. Isolation and identification of purulent bacteria from forest musk deer (*Moschus berezovskii*). Chin. J. Wildlife 33, 211–213 in Chinese, with English abstract.
Mitri, S., Foster, K.R., 2013. The genotypic view of social interactions in microbial communities. Annu. Rev. Genet. 47, 247–273.
Nealson, K.H., Platt, T., Hastings, J.W., 1970. Cellular control of the synthesis and activity of the bacterial luminescent system. J. Bacteriol. 104, 313–322.
Özkaya, Ö., Balbontín, R., Gordo, I., Xavier, K.B., 2018. Cheating on cheaters stabilizes cooperation in Pseudomonas aeruginosa. Curr. Biol. 28, 2070–2080 e6.
Pragman, A.A., Berger, J.P., Williams, B.J., 2016. Understanding persistent bacterial lung infections: clinical implications informed by the biology of the microbiota and biofilms. Clin. Pulm. Med. 23, 57–66.
Sandoz, K.M., Mitzimberg, S.M., Schuster, M., 2007. Social cheating in *Pseudomonas aeruginosa* quorum sensing. Proc. Natl. Acad. Sci. U. S. A. 104, 15876–15881.
Schuster, M., Lostroh, C.P., Ogi, T., Greenberg, E.P., 2003. Identification, timing, and signal specificity of *Pseudomonas aeruginosa* quorum-controlled genes: a transcriptome analysis. J. Bacteriol. 185, 2066–2079.
Short, F.L., Murdoch, S.L., Ryan, R.P., 2014. Polybacterial human disease: the ills of social networking. Trends Microbiol. 22, 508–516.
Tashiro, Y., Yawata, Y., Toyofuku, M., Uchiyama, H., Nomura, N., 2013. Interspecies interaction between *Pseudomonas aeruginosa* and other microorganisms. Microbes Environ. 28, 13–24.
Trapnell, C., Roberts, A., Goff, L., Pertea, G., Kim, D., Kelley, D.R., Pimentel, H., Salzberg, S.L., Rinn, J.L., Pachter, L., 2012. Differential gene and transcript expression analysis of RNA-seq experiments with TopHat and Cufflinks. Nat. Protoc. 7, 562–578.
West, S.A., Cooper, G.A., 2016. Division of labour in microorganisms: an evolutionary perspective. Nat. Rev. Microbiol. 14, 716–723.
West, S.A., Griffin, A.S., Gardner, A., Diggle, S.P., 2006. Social evolution theory for microorganisms. Nat. Rev. Microbiol. 4, 597–607.
Zhao, K., Liu, Y., Zhang, X., Palahati, P., Wang, H.N., Yue, B., 2011a. Detection and characterization of antibiotic resistance genes in *Arcanobacterium pyogenes* strains from abscesses of forest musk deer. J. Med. Microbiol. 60, 1820–1826.
Zhao, K., Li, X., Palahati, P., Zhang, X., Zeng, Bo., Yue, B., 2011b. Isolation and identification on pathogens of musk-deer abscess disease and antibiotic susceptibility assay. Sichuan J. Zool. 30, 522–526 in Chinese, with English abstract.
Zhao, K., Liu, M., Zhang, X., Wang, H., Yue, B., 2013. *In vitro* and *in vivo* expression of virulence genes in *Trueperella pyogenes* based on a mouse model. Vet. Microbiol. 163, 344–350.
Zhao, K., Li, Y., Yue, B., Wu, M., 2014. Genes as early responders regulate quorum-sensing and control bacterial cooperation in Pseudomonas aeruginosa. PLoS One 9, e101887.
Zhao, K., Zhou, X., Li, W., Zhang, X., Yue, B., 2016. Nutrient reduction induced stringent responses promote bacterial quorum-sensing divergence for population fitness. Sci. Rep. 6, 34925.
Zhao, K., Du, L., Lin, J., Yuan, Y., Wang, X., Yue, B., Wang, X., Guo, Y., Chu, Y., Zhou, Y., 2018. *Pseudomonas aeruginosa* quorum-sensing and type VI secretion system can direct interspecific coexistence during evolution. Front. Microbiol. 9, 2287.